Toxicology and Applied Pharmacology 300 (2016) 55–69

Contents lists available at ScienceDirect

Toxicology and Applied Pharmacology

journal homepage: www.elsevier.com/locate/ytaap

14-Deoxy-11,12-didehydroandrographolide induces DDIT3-dependent endoplasmic reticulum stress-mediated autophagy in T-47D breast carcinoma cells

Heng Kean Tan [a,b], Tengku Sifzizul Tengku Muhammad [a,c], Mei Lan Tan [a,b,*]

[a] Malaysian Institute of Pharmaceuticals & Nutraceuticals, National Institutes of Biotechnology Malaysia (NIBM), Ministry of Science, Technology & Innovation, Halaman Bukit Gambir, Pulau Pinang, Malaysia
[b] Advanced Medical & Dental Institute, Universiti Sains Malaysia, Pulau Pinang, Malaysia
[c] Institute of Marine Biotechnology, Universiti Malaysia Terengganu, Kuala Terengganu, Terengganu, Malaysia

ARTICLE INFO

Article history:
Received 27 January 2016
Revised 18 March 2016
Accepted 30 March 2016
Available online 2 April 2016

Keywords:
14-Deoxy-11,12-didehydroandrographolide
Endoplasmic reticulum stress
Autophagy
DDIT3/CHOP

ABSTRACT

14-Deoxy-11,12-didehydroandrographolide (14-DDA), a major diterpenoid isolated from *Andrographis paniculata* (Burm.f.) Nees, is known to be cytotoxic and elicits a non-apoptotic cell death in T-47D breast carcinoma cells. In this study, the mechanistic toxicology properties of 14-DDA in T-47D cells were further investigated. 14-DDA is found to induce the formation of endoplasmic reticulum (ER) vacuoles and autophagosomes, with concurrent upregulation of LC3-II in the breast carcinoma cells. It stimulated an increase in cytosolic calcium concentration and caused a collapse in mitochondrial membrane potential in these cells. In addition, both DDIT3 and GADD45A, molecules implicated in ER stress pathway, were significantly upregulated. DDIT3 knockdown suppressed the formation of both ER vacuoles and autophagosomes, indicating that 14-DDA-induced ER stress and autophagy is dependent on this transcription factor. Collectively, it is possible that GADD45A/p38 MAPK/DDIT3 pathway is involved in the 14-DDA-induced ER-stress-mediated autophagy in T-47D cells.

1. Introduction

14-Deoxy-11, 12-didehydroandrographolide (14-DDA) is isolated from a popular herbaceous plant known as *Andrographis paniculata* (Burm.f.) Nees (Acanthaceae). *A. paniculata* is a folk remedy used traditionally to treat a variety of ailments in Asian countries. The Indian Pharmacopoeia narrated it as a predominant constituent of at least 26 Ayurvedic formulations (Jarukamjorn and Nemoto, 2008) and it was listed as one of the medicinal plants in "The National List of Essential Drugs A.D. 1999" in Thailand (Pholphana et al., 2004). A variety of scientific evaluations have indicated that this plant and its derivatives have a broad range of pharmacological properties, including anti-tumor, antiviral and anti-inflammatory activities (Jayakumar et al., 2013). For example, 14-DDA is found to inhibit the HPV16 pseudo virus (HPV16PsV) infection with the highest potency as compared with other derivatives (Ekalaksananan et al., 2015). It has minimal toxic effects in A549 and BEAS-2B human lung epithelial cells and dose-dependently attenuated ovalbumin-induced airway eosinophilia, mucus production, pro-inflammatory biomarker expression in lung tissues and airway hyperresponsiveness. These results suggest that 14-DDA is probably safe but yet retains its useful pharmacological activities (Guan et al., 2011).

Studies on 14-DDA and other derivatives have been gaining a great deal of interest due to their potential therapeutic effects in multiple diseases. Andrographolide and 14-DDA, the two major constituents of the plant, showed promising cytotoxic activities on diverse cancer cells representing different types of human cancers (Tan et al., 2005; Lim et al., 2012; Tan et al., 2012). As one of the principle compound of *A. paniculata*, 14-DDA is more potent against breast carcinoma cells as compared with other diterpenoids such as andrographolide, andrographiside, neoandrographolide, deoxyandrographiside and 14-deoxy-12-methoxyandrographolide (Tan et al., 2005). 14-DDA is also found to have anti-proliferative activities on leukemia cell lines such as THP-1 and Jurkat. It also decreases the glutathione (GSH) content significantly and increases the expression of procaspase-3 in THP-1 cells, suggesting a redox-mediated cell death (Raghavan et al., 2014). In addition, 14-DDA is found to display potent preferential cytotoxicity against PANC-1 and PSN-1 human pancreatic cancer cells (Lee et al., 2015). Microscopic observation and flow cytometry analysis appear to indicate that 14-DDA triggers an apoptosis-like cell death (Lee et al., 2015). Despite this evidence, the mechanisms through which 14-DDA induces cell death remain unclear.

Previous microarray analysis revealed that 14-DDA upregulates tumor suppressor genes and downregulate genes that are normally overexpressed in cancers (Tan et al., 2012). In particular, three endoplasmic reticulum (ER) stress inducible genes, namely DNA-damage-inducible transcript 3/C/EBP homologous protein (*DDIT3/CHOP*),

* Corresponding author at: Advanced Medical and Dental Institute, Universiti Sains Malaysia, Pulau Pinang, Malaysia.
E-mail addresses: tanml@usm.my, drtanmelan@yahoo.com (M.L. Tan).

http://dx.doi.org/10.1016/j.taap.2016.03.017
0041-008X/

homocysteine-inducible, endoplasmic reticulum stress-inducible, ubiquitin-like domain member 1(*HERPUD1*) and DNA-damage-inducible transcript 4 (*DDIT4*), were significantly upregulated in 14-DDA-treated T-47D cells. Several mammalian target of rapamycin (mTOR)-regulated genes (*p27kip1*, *Myc* and *cyclin D1*) and mTOR pathway-related genes (*MXI1*, *FLCN*, *FNIP1*, *SFRS1* and *MCL1*) were also regulated (Tan et al., 2012). On the other hand, 14-DDA-treated breast carcinoma cells were highly vacuolated and extensively stained with monodansylcadaverine (Tan et al., 2012); thereby postulating that 14-DDA may induce the formation of either ER vacuole and/or autophagic vacuoles. Collectively, these results suggest that the effects of 14-DDA might be attributable to the regulation of ER stress and/or mTOR pathway. However, this has yet to be determined. Thus, the main aim of this study was to further investigate the mechanistic toxicology properties of 14-DDA in T-47D breast carcinoma cells.

2. Materials and methods

2.1. Materials

14-DDA was provided as described previously (Tan et al., 2005; Tan et al., 2012). Green fluorescent protein-LC3 (GFP-LC3) expression vector was a kind gift from Prof. Noboru Mizushima, Japan (Kabeya et al., 2000), while pDsRed2-ER vector was purchased from Clontech (USA). Cell culture medium and additives were purchased from either Gibco (USA) or Sigma-Aldrich (USA). Insulin-like growth factor 1 (IGF-1), rapamycin, 3-methyladenine (3-MA), chloroquine, thapsigargin, tunicamycin and dimethyl sulfoxide (DMSO) were obtained from Sigma-Aldrich (USA). Staurosporine and Akt Inhibitor VIII were purchased from Calbiochem (Germany). Anti-human antibodies against β-actin (ACTB), microtubule-associated protein-1 light chain 3A/B (LC3A/B), total mTOR, phospho-mTOR Ser2448, phospho-mTOR Ser2481, total Akt, phospho-Akt Ser473, immunoglobulin heavy chain binding protein (BiP), DDIT3, total protein kinase RNA-like ER kinase (total PERK), total eukaryotic translation initiator factor 2α (total eiF2α), phospho-eiF2α Ser51, total p38 mitogen-activated protein kinase (total p38 MAPK) and phospho-p38 MAPK Thr180/Tyr182 were all purchased from Cell Signaling Technology (USA). Anti-human phospho-PERK Ser713 antibody was from Biolegend (USA).

2.2. Cell culture and treatment

T-47D (ATCC® HTB-133™) breast carcinoma cells were purchased from American Type Culture Collection (ATCC®, USA) and cultured in RPMI 1640 medium supplemented with 10% (v/v) fetal bovine serum (FBS), 10 μg/ml bovine pancreas insulin, 100 units/ml penicillin and 100 μg/ml streptomycin. For mTOR signaling study, the culture medium was optimized to exclude bovine pancreas insulin during cell treatment. Depending on the type of experiments, T-47D cells were treated with either 4.5 μM 14-DDA [based on the LC_{50} concentration derived (Supplementary Fig. 1) and as mentioned in a previous study (Tan et al., 2012)] for 6 h–24 h or with various concentrations of 14-DDA (1.5 μM–13.5 μM) for 24 h. The cells were treated with tunicamycin (2.5 μg/ml for 6 h or 24 h), thapsigargin (1 μM for 24 h), staurosporine (1 μM for 4 h) or chloroquine (20 μM for 26 h) as control for either ER stress study or autophagic flux assay. The controls for mTOR signaling study were insulin-like growth factor 1 (IGF-1) (100 ng/ml for 0.5 h), rapamycin (1 μM for 24 h) and Akt Inhibitor VIII (20 μM for 24 h). Treatment duration and concentration for all controls were optimized prior to the actual experiments. T-47D cells were also treated with 0.1% (v/v) DMSO as vehicle control for 24 h. The final concentration of DMSO in all treatment conditions in this study did not exceed 0.1% (v/v).

2.3. Plasmid DNA transfection

T-47D cells were seeded into Lab-Tek chamber slides and transiently transfected with GFP-LC3 vector or pDsRed2-ER vector using Lipofectamine® LTX and PLUS™ Reagent (Invitrogen, USA) following the manufacturer's instruction. After 24 h of optimized transfection period, the cells were treated with 14-DDA and controls for 24 h. The cells were then fixed with paraformaldehyde and viewed under Carl Zeiss confocal laser scanning microscope 710 (Carl Zeiss, Germany). A minimum of 18 cells per sample was randomly selected. The number of GFP-LC3 punctate dots or pDsRed2-ER vacuoles per cell in GFP-LC3 or pDsRed2-ER positive cells was scored manually. Data are represented as mean of 18 cells of three independent experiments.

2.4. siRNA transfection and DDIT3 silencing

T-47D cells were transfected with 30 nM of ON-TARGETplus™ SMARTpool DDIT3 siRNA (siDDIT3) or ON-TARGETplus™ Non-targeting Pool siRNA (siControl) (Dharmacon, USA) using Lipofectamine® RNAiMAX Reagent (Invitrogen, USA) for 48 h (optimized condition). Subsequently, the cells were transfected with plasmid DNA (GFP-LC3 vector or pDsRed2-ER vector) for 24 h, treated and processed as described in the previous section. Data are represented as mean of 18 cells of three independent experiments.

2.5. Cell proliferation assay

Prior to the cell proliferation assay, T-47D cells were seeded onto two 96-well plates (T_0 and T_1). After 48 h, cells in T_0 plate were subjected to cell proliferation assay. Meanwhile cells in T_1 plate were treated with 14-DDA and controls. After 24 or 72 h, the cells in T_1 plate were subjected to cell proliferation assay using CellTiter 96® Aqueous One Solution Cell Proliferation Assay (Promega, USA) following the manufacturer's protocol. The absorbance was read at 490 nm using Envision® 2104 multilabel plate reader (PerkinElmer, USA). Subsequently, percentage of growth (%) was calculated using the formula as described by Boyd and co-workers (Boyd et al., 1992).

2.6. Determination of phosphatidylinositol 3-kinase (PI3K) activity using PI3 Kinase Activity/Inhibitor Assay Kit

The effects of 14-DDA on PI3K activity were examined using PI3 Kinase Activity/Inhibitor Assay Kit (Millipore, USA) according to the manufacturer's protocol and based on the principle that PI3K phosphorylates phosphatidylinositol-4.5-bisphosphate (PIP2), converting it to phosphatidylinositol-3,4,5-triphosphate (PIP3). It is a colorimetric assay and the absorbance value negatively correlates with the kinase activity. Briefly, the PI3 kinase reaction was set up in a glutathione-coated plate. 14-DDA (final concentration ranging from 3 nM to 3 mM) and wortmannin [known PI3K inhibitor at final concentration of 100 nM (Frederick et al., 2009)] were pre-incubated with PI3K isoforms (p110 α, β, δ or γ) for 10 min. This was followed by incubation in the reaction buffer containing PIP2 substrate, B-PIP3 and GRP-1/GST. The absorbance of the final solution was measured using EnVision® 2104 multilabel plate reader (PerkinElmer, USA) at 450 nm. Data are presented as relative percentage of samples to B-PIP3 control, as recommended in the manufacturer's protocol.

2.7. Determination of Akt1 kinase activity using AKT1 kinase enzyme system with ADP-Glo™ kinase assay

AKT1 kinase enzyme system with ADP-Glo™ kinase assay (Promega, USA) was used to determine if 14-DDA inhibits Akt1 kinase activity. It is a luminescence assay that measures Akt1 kinase activity by quantifying the amount of ADP produced during a kinase reaction. The luminescence signal positively correlates with ADP amount and kinase activity.

In brief, the kinase reaction was carried out in 384-well plate by incubating Akt1 kinase with 14-DDA (at final concentration of 3 nM–300 μM) for 10 min. Staurosporine (1 μM; general kinase inhibitor) was used as positive control (Meggio et al., 1995) whereas DMSO served as no inhibitor control. After incubation, ultra-pure ATP and Akt substrate were added and the plate was further incubated for 1 h. The kinase reaction was terminated by the addition of ADP-Glo™ reagent. Kinase detection reagent was used for the detection of ADP, followed by luminescence reading using EnVision® 2104 multilabel plate reader (PerkinElmer, USA). Net luminescence value was obtained by subtracting background luminescence value (no kinase control). Kinase activity was calculated by dividing the net test compound value by the net no inhibitor control value.

2.8. Western blot analysis

Total cellular protein was isolated using ProteoJET™ mammalian cell lysis reagent (Fermentas, Canada) supplemented with 1% (v/v) ProteoBlock™ protease inhibitor cocktail (Fermentas, Canada) and 1% (v/v) phosphatase inhibitor cocktail 3 (Sigma-Aldrich, USA). The proteins were then separated by SDS-PAGE and electrophoretically transferred to the PVDF membrane. After blocking, the membranes were probed with the indicated primary antibodies (at optimized dilution ratio) overnight and then incubated with IgG HRP-linked secondary antibody (1:1000) (Cell Signaling Technology, USA) for 3 h. The signal was detected using ECL™ Western blotting detection reagents (Amersham Biosciences, UK) and imaged on ChemiDoc™ XRS imaging system (Bio-Rad Laboratories, USA). Densitometric quantification of the bands was performed using Quantity One® 1-D analysis software (Bio-Rad Laboratories, USA). Protein expression was normalized against ACTB, which served as internal control of protein loading. Relative protein expression was then calculated by dividing the normalized intensity of treated sample by vehicle control.

2.9. Determination of c-jun N-terminal kinase (JNK) protein expression using InstantOne™ ELISA

InstantOne™ ELISA kit (eBioscience, USA) quantifies the protein expression of total JNK and phospho-JNK Thr183/Tyr185 based on the ELISA principle, where the absorbance signal positively correlates with the amount of target protein. Briefly, treated cells were lysed and then transferred to the InstantOne™ assay plate. Subsequently, the antibody cocktail was added and the plate was incubated for either 1.5 h (for detection of total JNK) or 3 h (for detection of phospho-JNK Thr183/Tyr185). Bound antibody complexes were detected using detection reagent and the absorbance signal was read at 450 nm using EnVision® 2104 multilabel plate reader (PerkinElmer, USA). Net absorbance value was obtained by subtracting background absorbance value (no lysate control). Relative protein expression was then calculated by dividing the net absorbance value of treated sample by vehicle control.

2.10. Measurement of cytosolic calcium concentration

Free cytosolic calcium concentration was measured using calcium sensitive fluorescent dye, Calcium Green™-1, acetoxymethyl (AM) ester (Molecular Probes, USA). Following cell treatment, T-47D cells were harvested and incubated with 1 μM Calcium Green™-1, AM ester for 20 min at room temperature. The cells were then washed with PBS/BSA buffer and analysed using BD Accuri™ C6 flow cytometer (BD Biosciences, USA). Relative fluorescence expression was calculated by dividing the FL1 signal (green fluorescence) of treated sample by vehicle control.

2.11. Measurement of mitochondrial membrane potential

Mitochondrial membrane potential was examined using BD™ MitoScreen flow cytometry mitochondrial membrane potential detection kit (BD Biosciences, USA) according to the manufacturer's protocol. Treated cells were trypsinized and stained with JC-1 dye for 10 min at 37 °C in CO_2 incubator. After washing with 1X assay buffer, the samples were analyzed by BD Accuri™ C6 flow cytometer (BD Biosciences, USA). Relative fluorescence expression was calculated by dividing the FL2/FL1 signal (red/green fluorescence) of treated sample by vehicle control.

2.12. Reverse transcription-quantitative real-time PCR (RT-qPCR)

Total RNA was isolated from the treated cells using QIAshredder™ and RNeasy® Mini Kit (Qiagen, Germany) according to the manufacturer's protocol. All primers were designed using Beacon Designer 7.80 (Premier Biosoft International, USA), except the primer for spliced X box-binding protein 1 (*XBP1*), which was obtained from a published paper (van Schadewijk et al., 2012). All primer sequences are listed in Table 1. The RT-qPCR reactions were performed using iScript™ one-step RT-PCR kit with SYBR® Green (Bio-Rad Laboratories, USA) in CFX96™ real-time PCR detection system (Bio-Rad Laboratories, USA). The thermal profile used for amplification was as follows: cycle 1 (cDNA synthesis), consisting of 10 min at 50.0 °C; cycle 2 (reverse transcriptase inactivation), consisting of 5 min at 95.0 °C; cycle 3 (PCR), consisting of 10 s at 95.0 °C followed by 30 s at optimized annealing temperature repeated for 40 cycles; and cycle 4 (melt curve analysis), consisting of 5 s at 65 °C–95 °C for 60 cycles, increasing by 0.5 °C for each cycle. The optimized primer annealing temperature for each gene is shown in Table 1. The RT-qPCR amplification efficiency for each set of primers was determined and computed into the Pfaffl mathematical model (Pfaffl, 2001) for subsequent calculation of relative gene expression.

2.13. Statistical analysis

Statistical comparisons for three independent experiments were performed using either one-way Anova with Dunnett's post-hoc test

Table 1
Primer sequences and optimized annealing temperature used for the RT-qPCR assay.

Gene symbol	GenBank accession no.	Nucleotide sequence	Amplification size (bp)	Annealing temperature (°C)
BiP	NM_005347	(F) 5′-TGAAGAAGTCTGATATTGATGAA-3′ (R) 5′-CCTTGCCATTGAAGAACT-3′	96	51.2
DDIT3	NM_004083	(F) 5′-TACTGACTACCCTCTCACTA-3′ (R) 5′-TGTCTACTCCAAGCCTTC-3′	77	54.1
GADD45A	NM_001924	(F) 5′-CGGTGATGGCATCTGAAT-3′ (R) 5′-GGAGTAACTGCTTGAGTAACT-3′	86	54.1
ATF4	NM_001675	(F) 5′-CGAATTAAGCACATTCCTCGATTCCAG-3′ (R) 5′-CATCTAAGAGACCTAGGCTTTCTTCAGC-3′	147	56.7
Spliced *XBP1*	NM_001079539	(F) 5′-TGCTGAGTCCGCAGCAGGTG-3′ (R) 5′-GCTGGCAGGCTCTGGGGAAG-3′	169	56.7
ACTB	NM_001101	(F) 5′-ATCACCATTGGCAATGAG-3′ (R) 5′-GATGGAGTTGAAGGTAGTT-3′	105	51.2–56.7

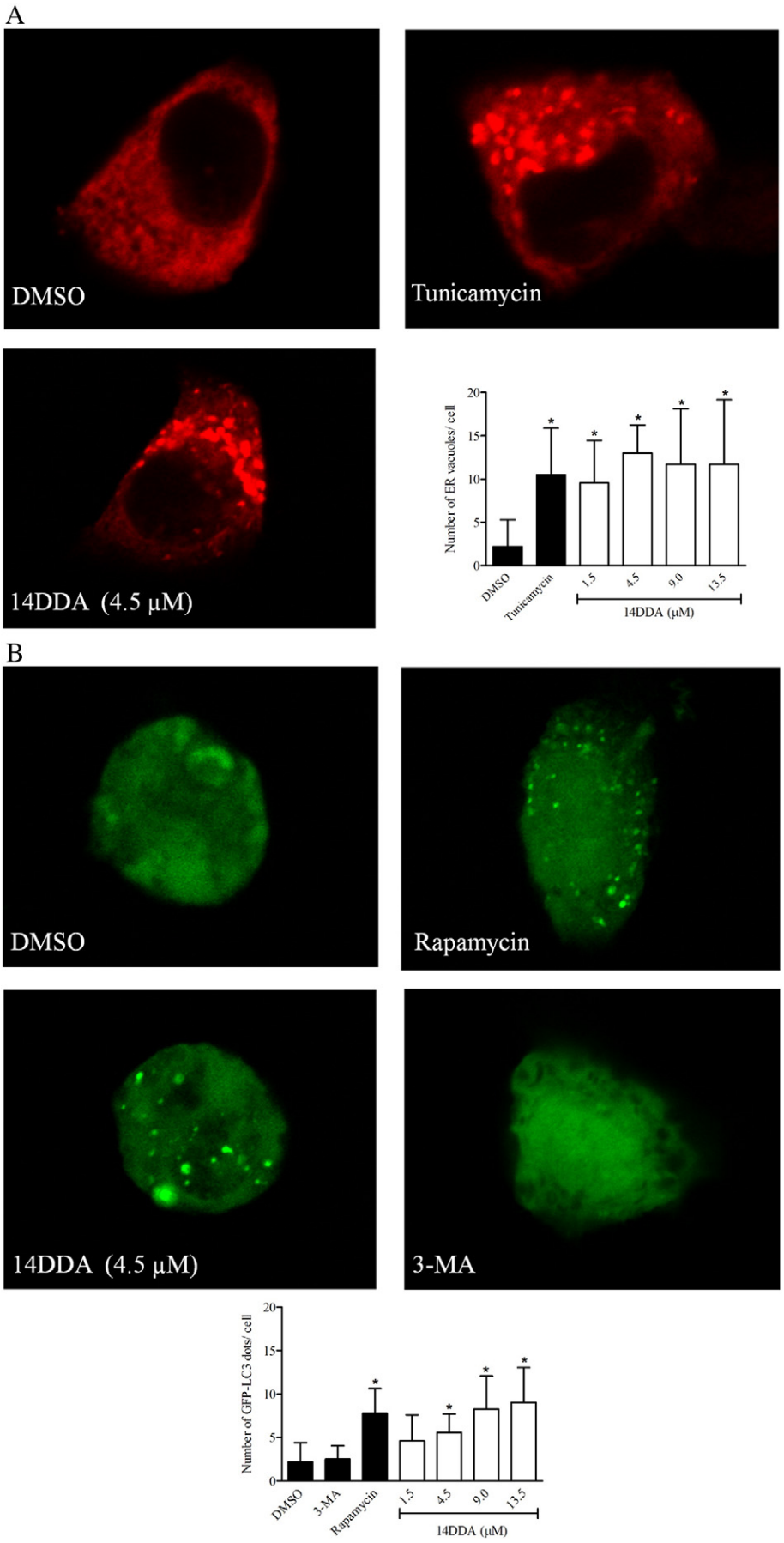
A
DMSO
Tunicamycin
14DDA (4.5 μM)
Number of ER vacuoles/ cell
20
15
10
5
0
DMSO
Tunicamycin
1.5
4.5
9.0
13.5
14DDA (μM)
B
DMSO
Rapamycin
14DDA (4.5 μM)
3-MA
Number of GFP-LC3 dots/ cell
20
15
10
5
0
DMSO
3-MA
Rapamycin
1.5
4.5
9.0
13.5
14DDA (μM)

or independent *t*-test (GraphPad Prism® software, version 5.0). Results are considered statistically significant if p value < 0.05.

3. Results

3.1. 14-DDA induced the formation of ER vacuoles and autophagosomes in T-47D breast carcinoma cells

To further characterize the identity of the vacuoles induced by 14-DDA, the effects of 14-DDA on the morphological changes of pDsRed2-ER vector- or GFP-LC3 vector-transfected cells were examined. The pDsRed2-ER expression vector encodes the ER targeting sequence of calreticulin and an ER retention signal (KDEL) fused to the red fluorescent protein. In normal cells, the marker will be localized diffusely, a pattern typical for the ER. However, in stress conditions, the DsRed-ER will be concentrated in discrete globular structures coinciding with ER vacuoles. In this study, a few ER vacuoles (approximately 2 ER vacuoles per cell) were observed in DMSO-treated T-47D cells (Fig. 1A), which was normal and represented the cell basal condition. As expected, 2.5 μg/ml tunicamycin as an ER stress inducer (Oslowski and Urano, 2011) produced an average of 10.5 vacuoles per cell. On the other hand, 14-DDA treatment for 24 h significantly induced the formation of ER vacuoles in T-47D cells, where the highest mean induction was observed at 4.5 μM. This data clearly indicated that 14-DDA induces ER dilatation, a morphologic feature of ER stress, in T-47D cells.

Rapamycin (1 μM; autophagy inducer) and 3-MA (10 mM; autophagy inhibitor) were used as controls for the autophagosome study (Tasdemir et al., 2008; Bauvy et al., 2009; Decuypere et al., 2013). As shown in Fig. 1B, the number of GFP-LC3 dots in 3-MA-treated cells was near to those observed in DMSO-treated T-47D cells. A significant increase in the number of fluorescence dots was observed when the cells were treated with rapamycin (an average of 7.8 dots per cell). Similarly, 14-DDA induced the number of dots in a concentration-dependent manner where significant induction was observed from 4.5 μM onwards. The highest induction was observed at 13.5 μM with an average of 9.1 dots per cell, suggesting that 14-DDA induces the formation of autophagosomes.

The level of LC3-II (lipidated and autophagosome-associated form of LC3) is one of the mainstays for autophagy detection (Barth et al., 2010). Western blot results showed a general increase in LC3-II levels in cells treated with various concentrations of 14-DDA with significant accumulation at the highest concentration of 13.5 μM (1.53 fold) (Fig. 1C). Autophagic flux assay was then performed to differentiate a true autophagy induction or rather, a block in the completion of the autophagic pathway by comparing LC3-II levels in the presence and absence of lysosomal inhibitors (Mizushima et al., 2010). Co-incubation with

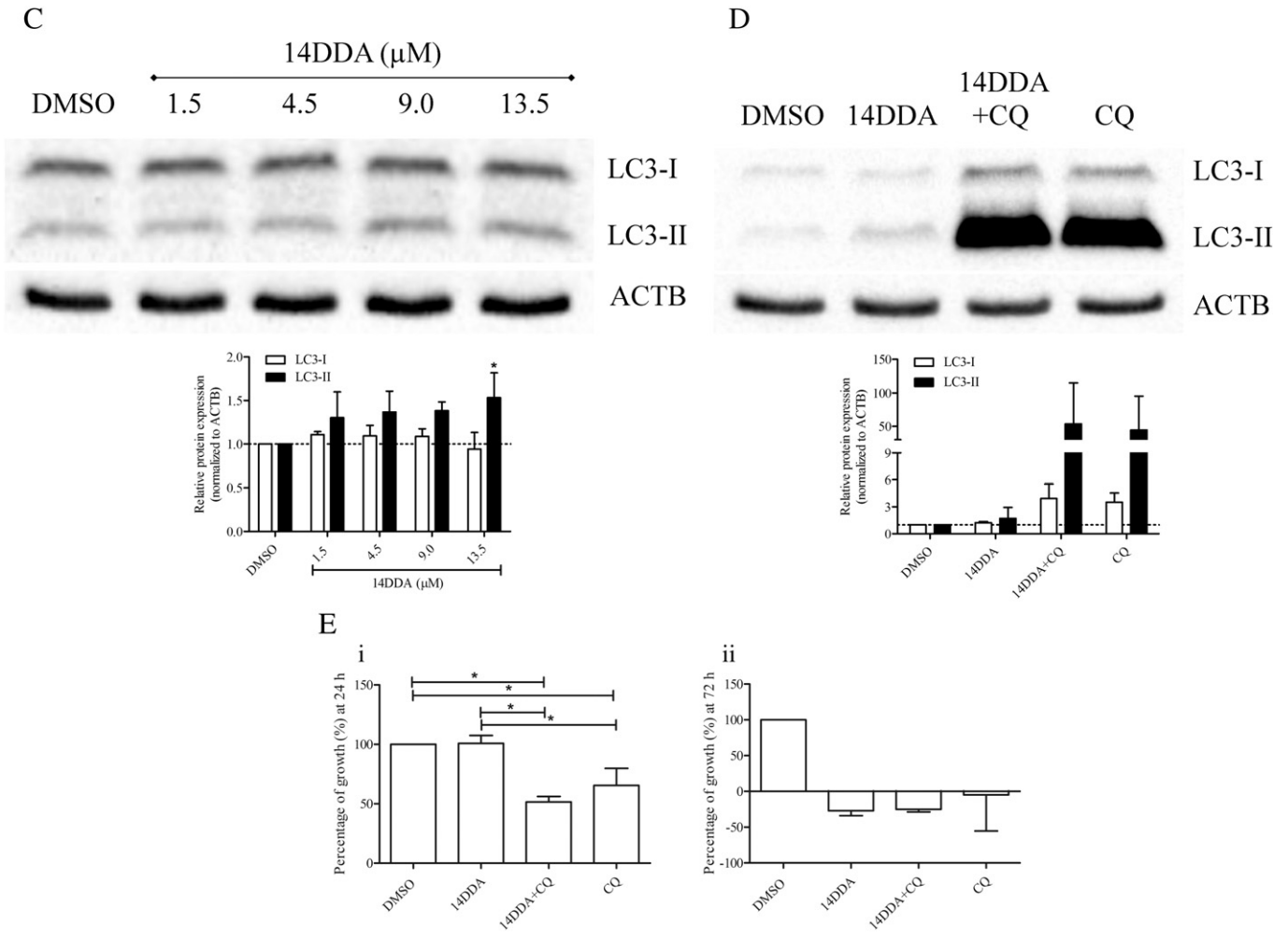

Fig. 1. 14-DDA induces the formation of ER vacuoles and autophagosomes in T-47D cells. T-47D cells were transiently transfected with (A) pDsRed2-ER vector or (B) GFP-LC3 vector before treated with 14-DDA for 24 h (C) Western blot analysis showing the protein expression of LC3-II in 14-DDA-treated cells for 24 h (D) T-47D cells were either treated with 4.5 μM 14-DDA alone for 24 h or after 2 h pretreatment with 20 μM chloroquine (CQ) (E) Cell proliferation assay of cells treated with 4.5 μM of 14-DDA and/or 20 μM of chloroquine at 24 h ($n = 3$) and 72 h ($n = 2$). Positive values (<100%) represent growth inhibition and negative values (<0%) represent cytotoxicity as compared with initial cells plated (T_0). Images shown are representative (magnification: 63× objective). Data are expressed as mean ± SD, $n = 3$. *$p < 0.05$ as compared with control.

chloroquine enhanced 14-DDA-induced accumulation of LC3-II to an average of 53.6-fold expression as compared with 1.72-fold expression in 14-DDA-treated cells or 44.7-fold in chloroquine-treated cells (Fig. 1D). Although the fold-expression differences between 14-DDA-chloroquine and chloroquine-treated cells were statistically insignificant, the differences between these two treatment arms averaged at

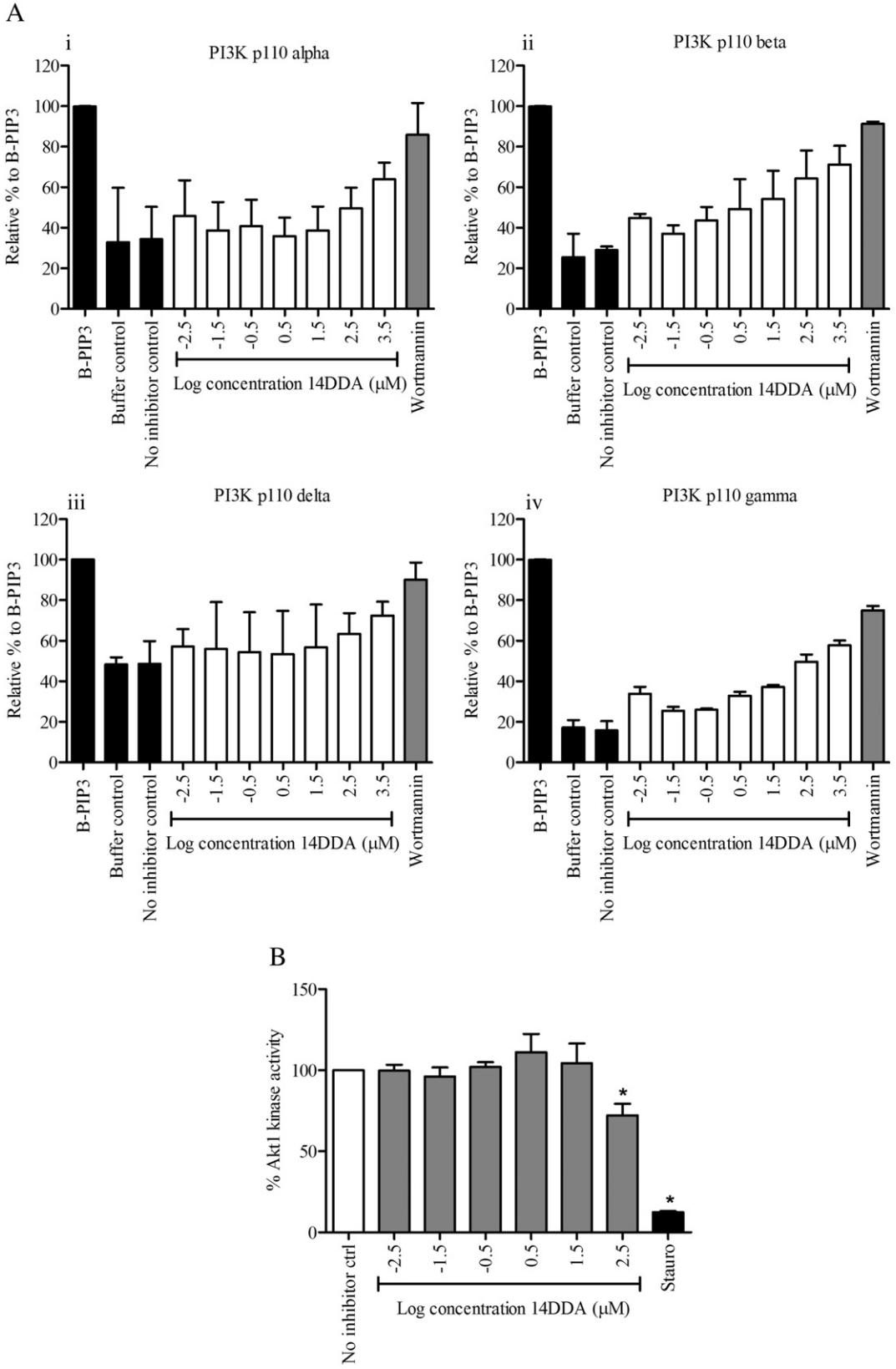

Fig. 2. 14-DDA is unlikely a PI3K or Akt1 inhibitor (A) The effects of 14-DDA (3 nM–3 mM) on PI3K isoforms. Data are expressed as mean of two independent experiments (B) Akt1 kinase activity was quantified by a luminescence assay by incubating 14-DDA (3 nM–300 μM) with Akt1 kinase. Results are expressed as mean ± SD, $n = 3$. *$p < 0.05$ compared with no inhibitor control (Stauro: Staurosporine).

9-fold. Thus, 14-DDA is much more likely in enhancing autophagy flux than blocking the pathway in these breast cells.

To determine if 14-DDA-induced autophagy is pro-death or pro-survival in function, cell proliferation assay was carried out. At 24 h, 14-DDA did not elicit immediate growth inhibition at 4.5 μM (the concentration used is approximate the LC_{50} value at 72 h), which was not surprising (Fig. 1E). However, the effect of chloroquine alone was moderately growth inhibitory, and combination of both chloroquine and 14-DDA induced significant growth inhibition. Although the effects of autophagy appeared to be pro-survival at 24 h, the growth inhibition may be due to chloroquine and not the direct effects of autophagy inhibition. Prolonging the treatment duration to 72 h further enhanced the cytotoxic activities of 14-DDA and/or chloroquine against the cells (Fig. 1E). Autophagy inhibition have no pronounced effects on the cytotoxic activities of 14-DDA at 72 h. Chloroquine alone also produced cell toxicity at 72 h, indicating the toxicity exerted by 14-DDA in the presence of chloroquine may be a result of additive effects.

3.2. 14-DDA-induced cell death is independent of PI3K/Akt/mTOR signaling pathway

Since PI3K/Akt/mTOR pathway is the main regulatory pathway that negatively regulates autophagy and several mTOR-related genes were regulated in our previous study (Kondo et al., 2005; Tan et al., 2012; Wojcik, 2013), the next goal was to determine if the resultant autophagy was due to inhibition of this pathway. PI3 kinase assay was performed to investigate if 14-DDA inhibits the p110 catalytic subunits of PI3K. Surprisingly, no clear inhibition trend was observed for both α and δ isoforms (Fig. 2A). 14-DDA at the highest concentration of 3 mM produced <80% inhibition. Although a dose-dependent effect was observed for β and γ isoforms, inhibition also did not exceed 80% at the highest concentration (Fig. 2A). As for the positive control, wortmannin at 100 nM inhibited at least 80% of the lipid kinase activity of these isoforms.

The extent of inhibitory effect of 14-DDA on Akt1 kinase activity was then examined. 14-DDA did not inhibit Akt1 kinase activity at low concentrations (3 nM to 30 μM) (Fig. 2B). Only the highest concentration of 300 μM produced a significant reduction of Akt1 kinase activity to approximately 72.2% as compared with control. On the other hand, staurosporine (1 μM; general kinase inhibitor) inhibited the Akt1 kinase activity to 12.5%, as expected. Taken together, 14-DDA has weak PI3K and Akt1 kinase inhibitory activities.

To further examine whether 14-DDA inhibits Akt/mTOR pathway in cultured cells, T-47D cells were treated with 14-DDA (1.5–13.5 μM) for 24 h, followed by Western blot analysis. As expected, IGF-1 (mTOR pathway inducer) stimulated phosphorylation of Akt at Ser473 and

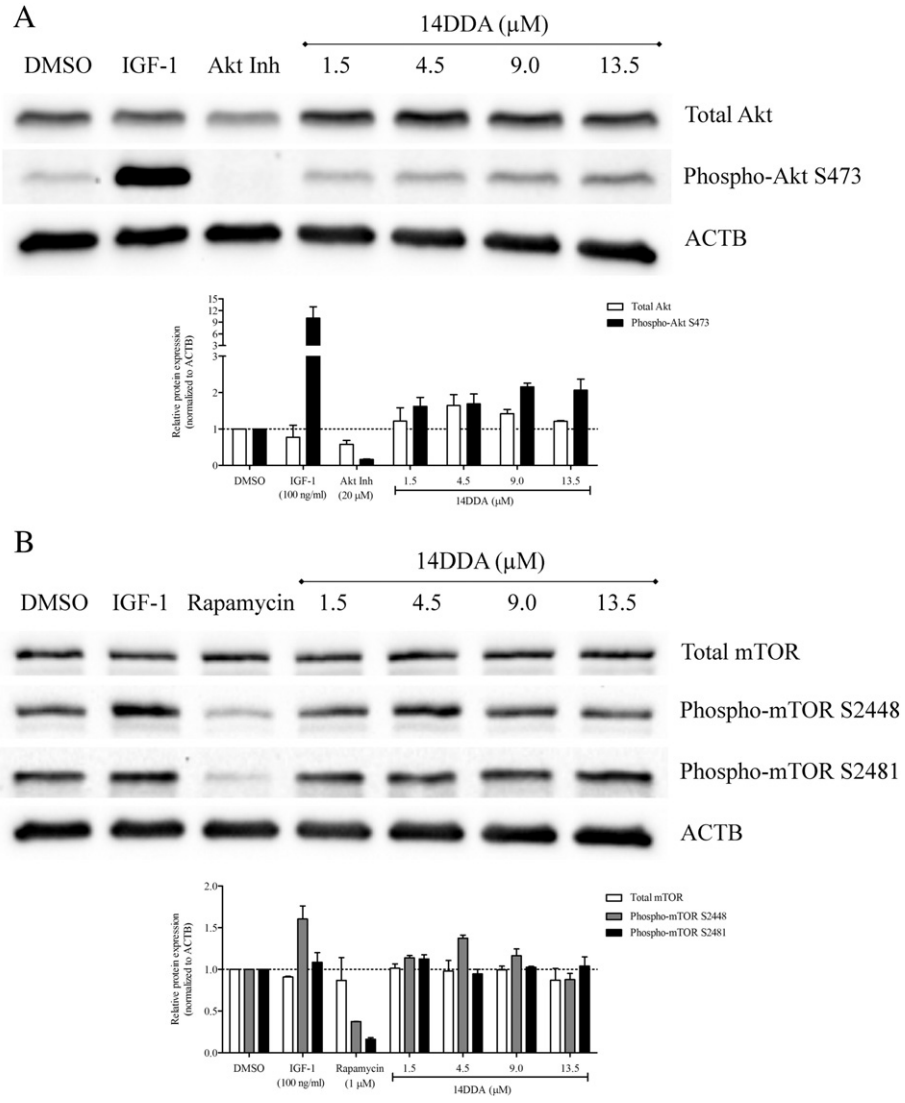

Fig. 3. 14-DDA did not inhibit Akt/mTOR pathway in T-47D cells. The effects of 14-DDA on the expression of (A) total Akt and phospho-Akt (B) total mTOR and phospho-mTOR proteins in T-47D cells. Western blot results are representative of typical blots and densitometric data are expressed as mean of two independent experiments (Akt Inh: Akt Inhibitor VIII).

mTOR at Ser2448 (Akt-mediated phosphorylation site (Tan et al., 2014)) (Fig. 3A, B). On the other hand, Akt Inhibitor VIII inhibited the protein expression of total Akt and phospho-Akt Ser473 (Fig. 3A). Likewise, 1 μM of rapamycin inhibited the phosphorylation of mTOR at both phosphorylation sites (Fig. 3B). Interestingly, 14-DDA did not inhibit the phosphorylation of Akt/mTOR or the total Akt/mTOR protein levels (Fig. 3A, B). By contrast, 14-DDA at certain concentrations appeared to induce the phosphorylation of Akt and phospho-mTOR Ser2448. These results indicated that 14-DDA-induced cytotoxicity is unlikely caused by the inhibitory effect of 14-DDA on the Akt/mTOR signaling pathway.

3.3. 14-DDA increases the cytosolic calcium concentration and disrupts the mitochondrial membrane potential in T-47D cells

To further characterize the 14-DDA-induced cytotoxicity, treated cells were loaded with Calcium Green-1, AM ester and JC-1 dye to measure changes in cytosolic calcium concentration and mitochondrial membrane potential, respectively, using flow cytometry. The increase in cytosolic calcium concentration after 14-DDA (4.5 μM) treatment was observed starting at 6 h (Fig. 4A). The increase was gradual and significant induction was observed at 18 h and 24 h. Thapsigargin (1 μM), which is a SERCA inhibitor, also significantly elevated cytosolic calcium concentration to 1.72 fold relative to vehicle-treated control (Fig. 4A). On the other hand, staurosporine significantly decreased JC-1 red/green fluorescence intensity ratio to 0.58-fold (Fig. 4B). However, only cells exposed to 4.5 μM 14-DDA for 24 h caused a significant decrease in the ratio, representing an increase number of cells with depolarized mitochondria. Thus, 14-DDA clearly disrupts intracellular calcium homeostasis and mitochondrial membrane potential, which are associated with ER stress.

3.4. 14-DDA induces ER stress markers in T-47D cells

Evidence of ER stress was further supported by the gene and protein expression studies on ER stress markers (Fig. 5, Fig. 6A–B). As estimated, exposure of cells to 2.5 μg/ml tunicamycin for 24 h resulted in a marked increase in the mRNA and protein expression of most ER stress markers (Figs. 5, 6A–B). Although the mRNA expression of BiP was slightly induced by 14-DDA (4.5 μM) at 24 h (1.38 fold) (Fig. 5), BiP protein expression was not significantly upregulated over 6–24 h (Fig. 6A, B). On the other hand, significant upregulation of DDIT3 mRNA expression was observed from 6 h (2.12 fold) to 18 h (2.62 fold) (Fig. 5). The protein expression of DDIT3 was also significantly induced at all time points, with the most prominent induction effect at 6 h (1.79 fold) (Fig. 6B).

To further characterize the mechanism of ER stress induction, two primary canonical arms of UPR signaling (PERK pathway and IRE1 signaling) were examined. As shown in Fig. 6B, 14-DDA slightly upregulated the protein expression of phospho-PERK Ser713 starting from 6 h onwards but effects on total PERK was negligible. Minimal induction of phospho-eiF2α Ser51 was observed at 24 h (1.30 fold) (Fig. 6B). Quite predictably, tunicamycin induced the protein phosphorylation and mRNA expression of most ER stress molecules, except for the phosphorylation of PERK in these breast cells (Fig. 6B). On the other hand, ATF4 mRNA expression was stimulated upon 14-DDA exposure, where the most significant induction was observed at 24 h with 1.58 fold increase (Fig. 5).

Monitoring XBP1 splicing status by RT-qPCR represents a reliable indirect method to determine inositol-requiring enzyme 1(IRE1) activation (Hiramatsu et al., 2011; Oslowski and Urano, 2011). Our results indicated that 14-DDA did not affect the mRNA expression of spliced XBP1 (Fig. 5). Interestingly, growth arrest and DNA damage inducible alpha (GADD45A) mRNA expression increased in time-dependent manner and significant induction was observed at 6 h (1.29 fold), 12 h (1.52 fold) and 24 h (1.96 fold). On the same note, 14-DDA treatment significantly induced the phosphorylation of p38 MAPK in time-dependent manner (Fig. 6B). In addition, there was a slight phosphorylation of JNK protein only at 6 h based on the ELISA kit (Fig. 6C). However, when the treatment period increased, the phosphorylation of JNK protein gradually decreased to basal level at 24 h. Based on these observations, it is possible that GADD45A/p38 MAPK/DDIT3 pathway is involved in the 14-DDA-induced ER-stress. However, the role of PERK, eiF2α, ATF4 and JNK remain unclear.

3.5. DDIT3 knockdown suppressed the formation of ER vacuoles and autophagosomes in 14-DDA-treated T-47D cells

DDIT3 is an ER stress-inducible transcription factor that is critical in supporting ER-stress induced autophagy and it has been identified as the key player in mediating the anti-tumor effects of ER stress-inducing agents (Rouschop et al., 2010; Avivar-Valderas et al., 2011; B'Chir et al., 2013; Schonthal, 2013). To determine if DDIT3 mediates the 14-DDA-induced ER stress, the expression of DDIT3 was knocked-down using DDIT3 siRNA (siDDIT3), followed by morphological examination using ER and autophagosome markers. Transfection of siDDIT3 in T-47D cells effectively downregulated DDIT3 mRNA and protein levels (Supplementary Fig. S3) and double transfection produced a small difference in basal cell viability as examined using trypan blue exclusion test (Supplementary Fig. S2). Approximately 3.1–4.5 ER vacuoles/cell

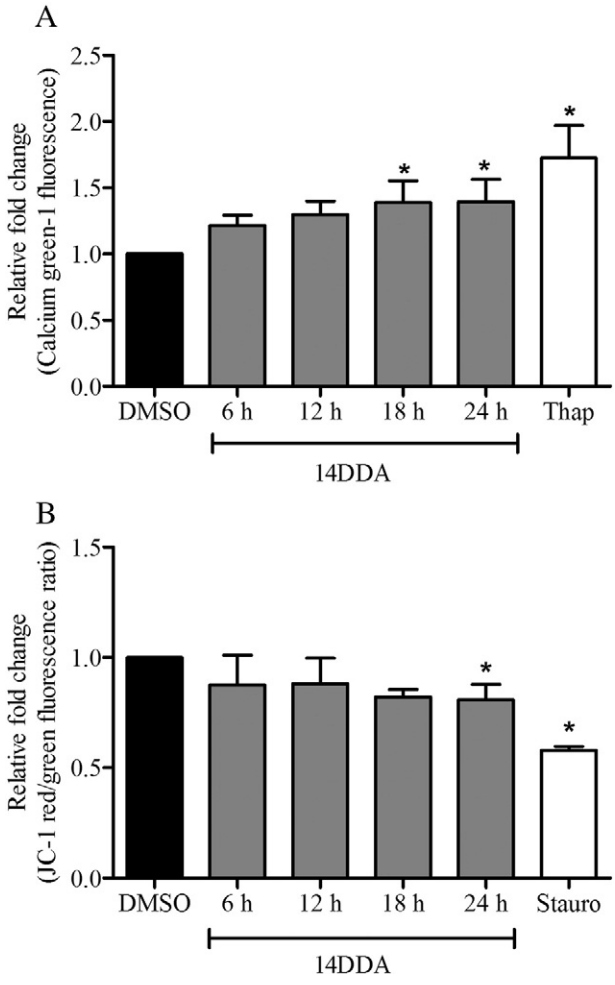

Fig. 4. 14-DDA increases cytosolic calcium concentration and disrupts mitochondrial membrane potential in T-47D cells. (A) Cytosolic calcium levels in cells treated with 14-DDA (4.5 μM) at different durations. Cells were stained with Calcium Green™-1, AM ester and then analysed using flow cytometry (B) Depolarization of mitochondrial membrane potential in cells treated with 14-DDA (4.5 μM) as shown by the decrease in JC-1 red/green fluorescence ratio. Results are expressed as mean ± SD, $n = 3$. $^*p < 0.05$ compared with control (Thap: Thapsigargin; Stauro: Staurosporine).

was observed in vehicle-treated cells silenced with either siDDIT3 or siControl (Fig. 7A), which were slightly higher than those observed in Fig. 1A, indicating that double transfection might have imposed additional stress on the cells. As expected, 14-DDA induced the formation of ER vacuoles in siControl-transfected cells (9.3 vacuoles) but not in siDDIT3-transfected cells (2.9 vacuoles), suggesting that ER stress induction is likely dependent on the expression of this transcription factor.

Having confirmed that DDIT3 is an important mediator for ER stress induction in 14-DDA-treated cells, we next examined whether DDIT3 may also play a role in 14-DDA-induced autophagosomes. As shown in Fig. 7B, 14-DDA induced an average of 5.1 GFP-LC3 dots/cell in siControl-transfected cells, a higher number as compared with the vehicle-treated siControl-transfected cells. The number of dots per cell was reduced to an average of 3.7 in the 14-DDA and siDDIT3-treated cells, implying that 14-DDA-induced autophagosomes are possibly mediated by DDIT3 as well. Similar with 14-DDA, knockdown of DDIT3 also blocked autophagosome formation induced by rapamycin (Fig. 7B). Based on these data, both 14-DDA-induced ER stress and autophagy are likely dependent on DDIT3 expression.

4. Discussion

14-DDA is reported to elicit a non-apoptotic type of cell death in T-47D breast carcinoma cells (Tan et al., 2005). Subsequently, a microarray analysis has identified a subset of transcripts with roles in ER stress response and mTOR signaling significantly regulated in these cells (Tan et al., 2012). Many cellular processes including apoptosis, autophagy and energy metabolism are controlled by either ER stress pathway [also known as unfolded protein response (UPR)] or mTOR signaling pathway. Interestingly, the crosstalk between these two signaling pathways has been identified only recently (Appenzeller-Herzog and Hall, 2012). ER stress is known to negatively regulate Akt/TSC/mTOR pathway to enhance autophagy-mediated cell death (Qin et al., 2010). In

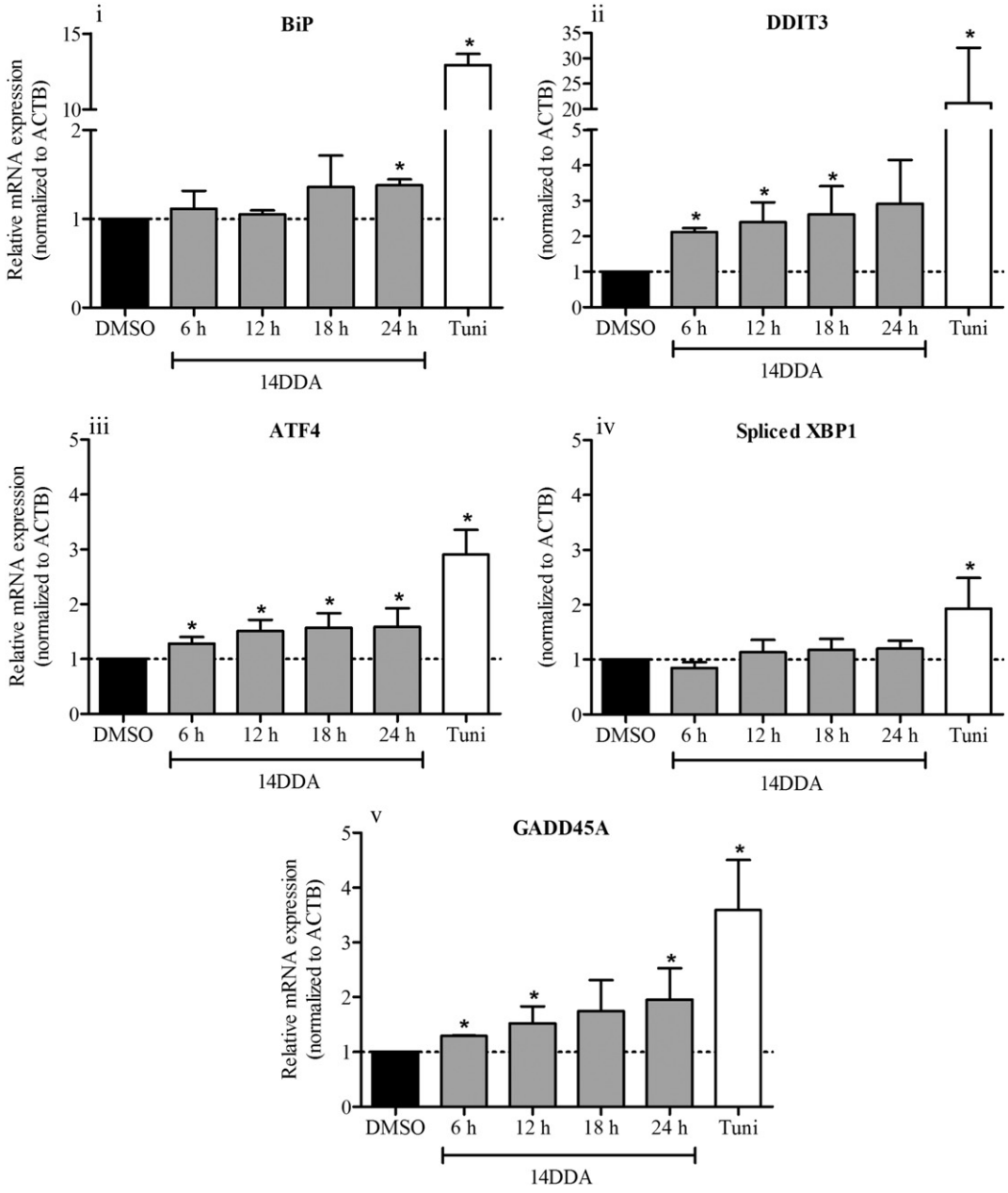

Fig. 5. 14-DDA induces the mRNA expression of ER stress molecules such as *DDIT3* and *GADD45A* for >2-fold changes. T-47D cells were incubated with 14-DDA (4.5 μM) for different time intervals and subjected to RT-qPCR. Data are presented as mean ± SD, $n = 3$. $^{*}p < 0.05$ compared with control (Tuni: Tunicamycin).

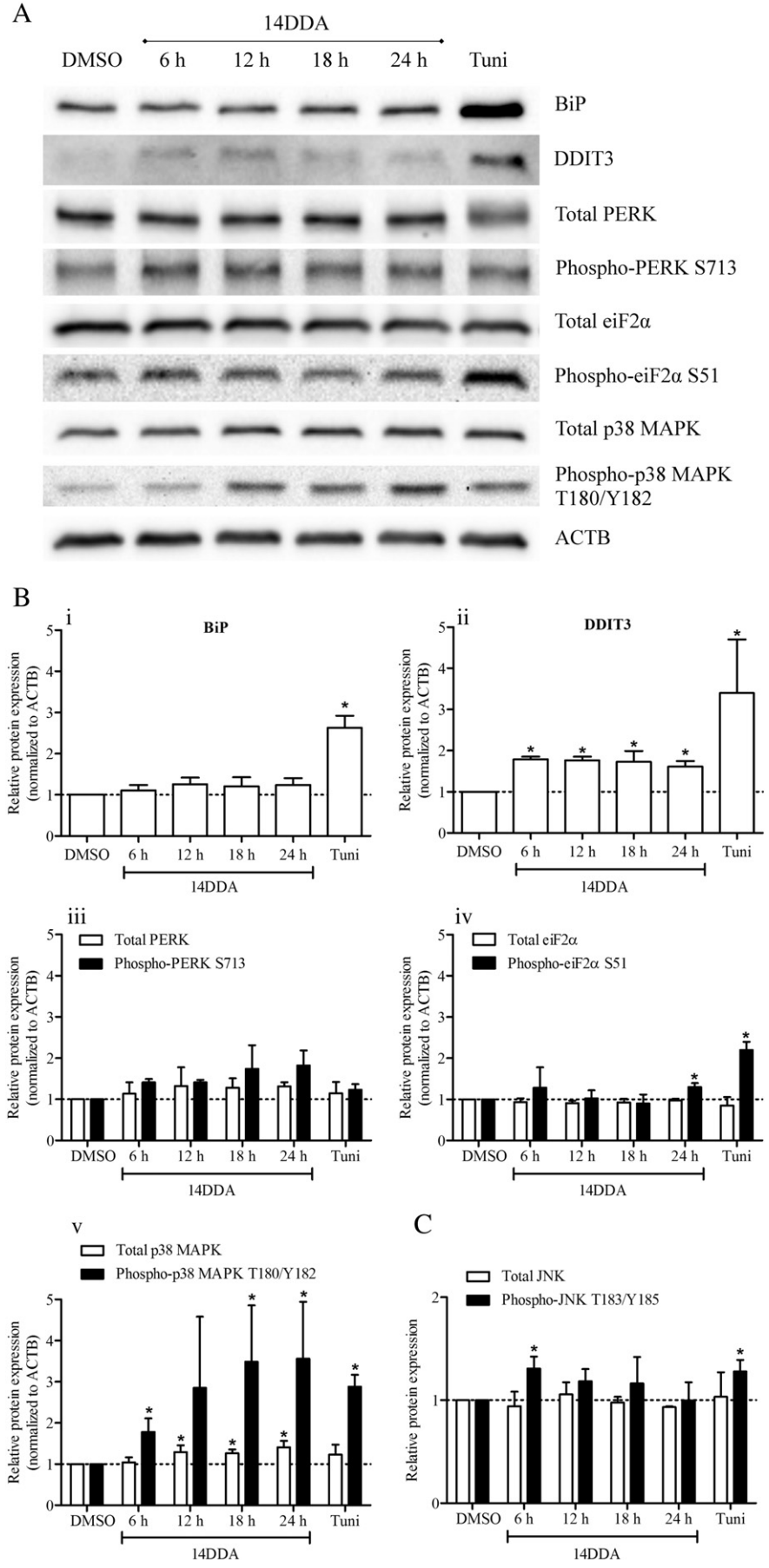
A
14DDA
DMSO
6 h
12 h
18 h
24 h
Tuni
BiP
DDIT3
Total PERK
Phospho-PERK S713
Total eiF2α
Phospho-eiF2α S51
Total p38 MAPK
Phospho-p38 MAPK T180/Y182
ACTB
B
i
BiP
ii
DDIT3
iii
Total PERK
Phospho-PERK S713
iv
Total eiF2α
Phospho-eiF2α S51
v
Total p38 MAPK
Phospho-p38 MAPK T180/Y182
Relative protein expression (normalized to ACTB)
C
Total JNK
Phospho-JNK T183/Y185
Relative protein expression

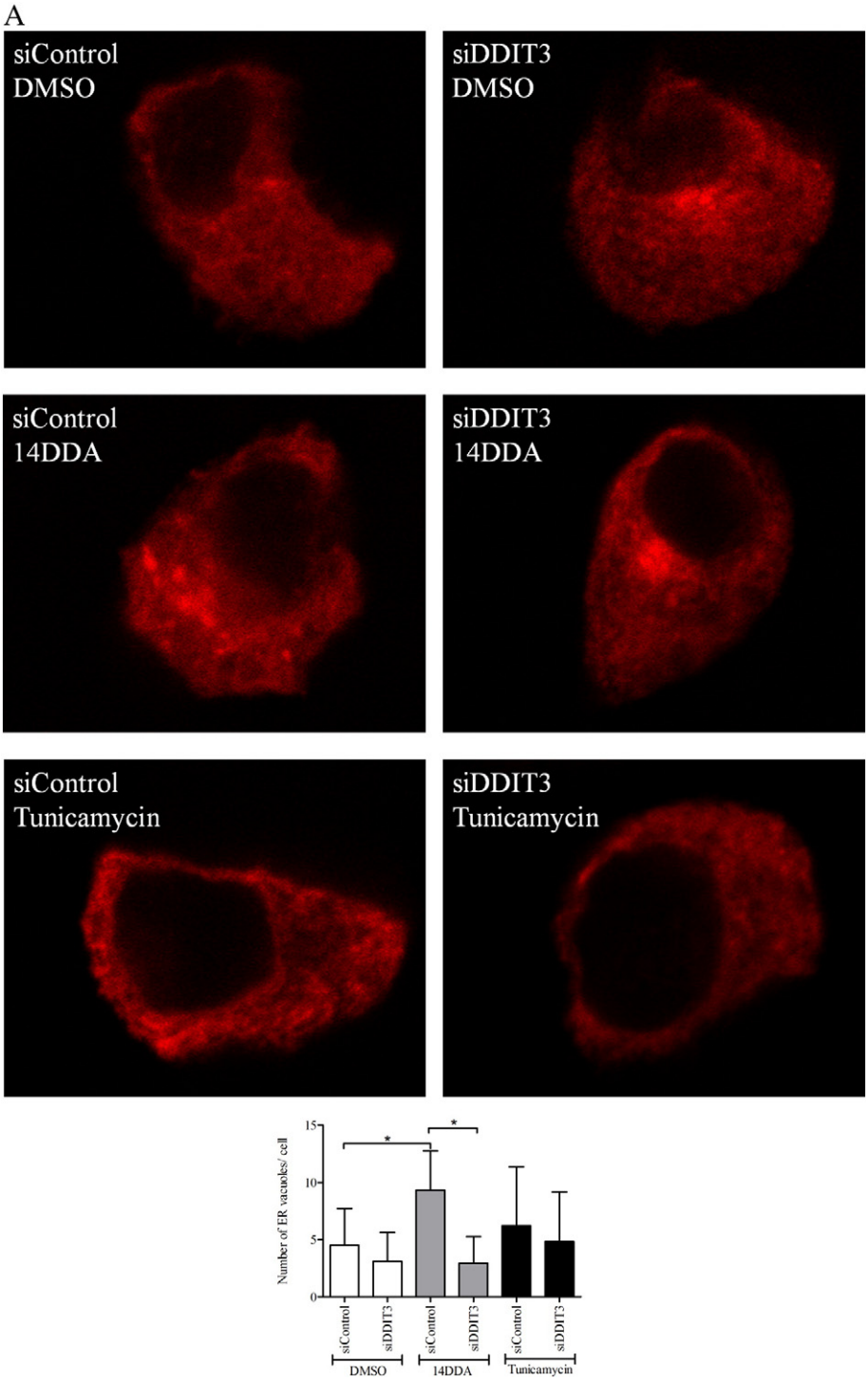

Fig. 7. DDIT3 knockdown suppressed the formation of ER vacuoles and autophagosomes in 14-DDA-treated T-47D cells. Cells were transfected with DDIT3 siRNA (siDDIT3) or control siRNA (siControl) for 48 h, before transfected with (A) pDsRed2-ER vector or (B) GFP-LC3 vector for 24 h. Confocal microscopy images are representative (magnification: 63× objective). Data are expressed as mean ± SD, $n = 3$. $^{*}p < 0.05$ compared with control.

addition, DDIT3 has been shown to mediate ER stress-induced autophagy via inhibition of the Akt/mTOR pathway (Salazar et al., 2009). Though it was earlier hypothesized that 14-DDA could induce ER stress and/or autophagy in T-47D cells probably via the mTOR pathway, the results suggested otherwise.

14-DDA was found to induce the formation of autophagosomes and accumulation of LC3-II in T-47D breast carcinoma cells. This was fairly consistent with our previous study (Tan et al., 2012). Although autophagic flux assay could not determine for sure if the accumulation of autophagosomes were due to dynamic autophagy or blocking of the

Fig. 6. 14-DDA triggers the expression of ER stress proteins in T-47D cells (A) Image is representative of the Western Blot analysis of ER stress proteins (B) Densitometric analysis of BiP, DDIT3, PERK, eiF2α and p38 MAPK (C) Total JNK and phospho-JNK Thr183/Tyr185 protein levels were examined by ELISA kit. Data for all proteins are expressed as mean ± SD ($n = 3$). $^{*}p < 0.05$ compared with control except for PERK. No statistical analysis were performed for PERK ($n = 2$) (Tuni: Tunicamycin).

pathway, based on the LC3-II fold expression differences between chloroquine-treated and 14-DDA-chloroquine-treated cells, 14-DDA is much more likely in enhancing autophagy flux than the latter.

The autophagy process elicited by 14-DDA appears to be pro-survival at 24 h, however, the same cannot be said when the duration of exposure was extended to 72 h. Chloroquine treatment alone induced growth inhibition as early as 24 h and exerted cytotoxicity at 72 h, further complicated the role of autophagy inhibition in this experiment. Interestingly, the cytotoxic activities of 14-DDA was not affected significantly in the presence or absence of the autophagy inhibitor at 72 h, indicating that either 14-DDA is capable of circumventing the effects of autophagy inhibition or that the overall cytotoxic effects were additive. Thus, 14-DDA-induced autophagy appears to be protective at 24 h but remain inconclusive at later stages. Interestingly, chloroquine may not be a suitable choice to be used as an autophagy inhibitor in certain cell types due to its toxicity.

Autophagy is a multi-step process, and various signaling pathways have been implicated in its up- or down-regulation. There are multiple evidences which indicated that the PI3K/Akt/mTOR pathway activated in various cancers represents the major regulatory mechanism of

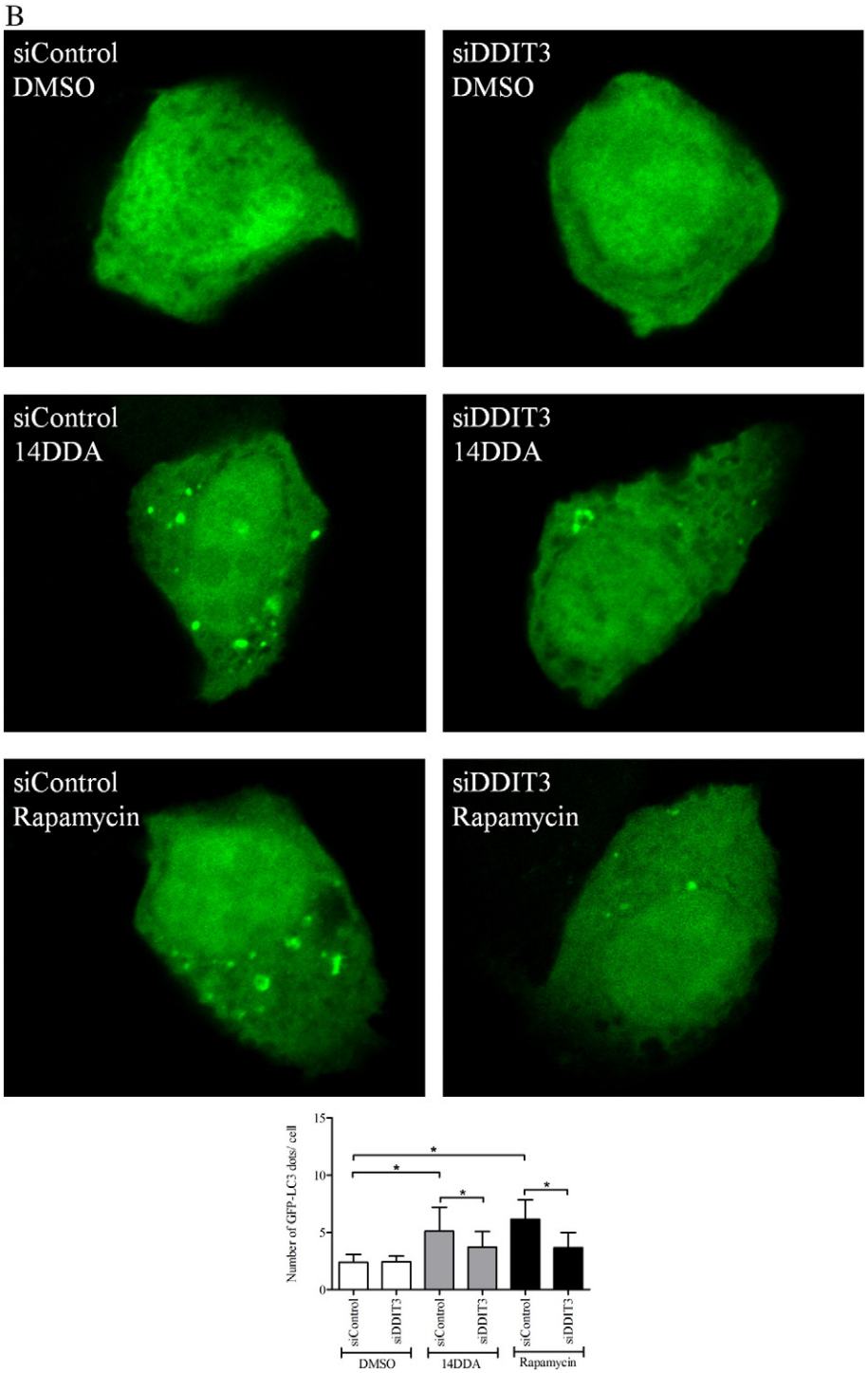

Fig. 7 (*continued*).

autophagy (Kondo et al., 2005; Wojcik, 2013). Class I PI3Ks are heterodimers composed of a regulatory subunit and a p110 α, β, δ or γ catalytic subunit (Liu et al., 2009; Rodon et al., 2013). In this study, 14-DDA's activity on all isoforms was negligible and inhibition of PI3K isoforms hardly achieves 80% at the highest concentration of 3 mM. Most PI3K inhibitors in the clinical trials have IC_{50} values at nanomolar concentration (Yap et al., 2008). Although a dose-dependent effect was observed for p110 γ isoform, a promising target for inflammatory and autoimmune diseases, inhibition did not exceed 60% at the highest concentration.

Akt, a downstream effector of PI3K, is a serine/threonine protein kinase involved in tumor growth, cancer cell invasion and chemoresistance (Park et al., 2005; Fortier et al., 2011). In this study, 14-DDA is unlikely to be an Akt inhibitor based on the luminescence assay. Consistent with the cell-free kinase assays, 14-DDA also did not inhibit the Akt/mTOR pathway proteins in T-47D cells (Fig. 3). By contrast, the protein expression of total Akt and phospho-Akt Ser473 was induced in these cells. The activation of Akt might be due to indirect feedback activation effects as signaling pathways are neither linear nor unidirectional and are regulated by compensatory feedback mechanisms that allow cell survival (Garber, 2009; Liu et al., 2009). For example, inhibition of mTOR activity by rapamycin is found to activate Akt and eIF4E survival pathways (Sun et al., 2005; O'Reilly et al., 2006; Wan et al., 2007). Although Akt activation may contribute to cancer progression, it has been shown that activation of Akt alone is insufficient for tumorigenesis or cell survival, where additional signals are required (Fayard et al., 2005; van Gorp et al., 2006). Akt activation is known to occur in response to various cellular stresses such as heat shock, hyperosmolarity, oxidative stress and chemical stressors (Konishi et al., 1996; Konishi et al., 1997; Pal and Mandal, 2012). Thus, it is possible that Akt activation in T-47D cells was due to cellular stress elicited by 14-DDA.

In addition to PI3K/Akt/mTOR signaling, ER stress signaling pathway has been implicated in the regulation of autophagy (Wojcik, 2013). ER stress not only induces autophagy via inhibition of the mTOR signaling pathway, but also directly regulates autophagy process through the ER stress transcription factors such as ATF4 and DDIT3 (Verfaillie et al., 2010; B'Chir et al., 2013). Autophagy is initially induced to eliminate abnormal protein aggregates and damaged ER. As such, the autophagy induction is a protective response to the overload of unfolded or misfolded proteins (Woehlbier and Hetz, 2011; Hetz, 2012). However, if the ER stress is unresolved, over-activation of the autophagy process will eventually result in autophagy associated cell death. Thus, autophagy plays an important role in the life-and-death decisions of the ER stress response (Schonthal, 2009).

The ability of cells to respond to perturbations in ER function is critical for cell survival, but chronic or unresolved ER stress can lead to cell death (Verfaillie et al., 2010; Tabas and Ron, 2011). In view that ER stress is basally activated in many cancers, induction of ER stress that aggravates the pre-existing ER stress condition and the subsequent activation of autophagy is an attractive cancer therapeutic strategy (Schleicher et al., 2010). In addition, since most normal cells are not subjected to stress, moderate intensity ER stress inducer exerts tumor-selective cytotoxic outcome by aggravating ER stress in tumor cells, but only modestly triggers ER stress in normal cells (Healy et al., 2009; Schonthal, 2009). The effectiveness of chemotherapeutics is usually diminished by the fact that they induce toxicity to both normal and cancer cells (Turcotte and Giaccia, 2010). Thus, the feasibility of moderate intensity ER stress inducer to produce tumor-selective cytotoxic outcome represents an alternative therapeutic target to improve cancer therapy. In fact, many anti-cancer compounds have been reported to act via ER stress induction and some of them are currently in clinical trials (Nawrocki et al., 2005; Salazar et al., 2009; Schonthal, 2009; Quan et al., 2010; Galluzzi et al., 2012; Schonthal, 2013), indicating that the induction of ER stress in cancer cells is a therapeutic possibility.

Although 14-DDA is unlikely an mTOR pathway inhibitor, our subsequent findings demonstrated that it is an ER stress inducer. ER is a major intracellular reservoir of calcium ions and plays a central role in cellular calcium homeostasis. Perturbation in ER function is known to cause leakage of calcium ions from the ER lumen to the cytosol, leading to disruption in mitochondrial membrane potential and eventually cell death (Kroemer et al., 2007; Verfaillie et al., 2010). Based on this study, 14-DDA most likely triggers expansion of ER membrane into vacuoles, cytosolic calcium elevation and mitochondrial membrane depolarization, all of which are indicative of ER stress. Subsequently, elucidation of the pathway revealed that 14-DDA activates the GADD45A/p38 MAPK/DDIT3 pathway but independent of BiP and spliced XBP1. Either the mRNA or protein expression of these molecules in this pathway showed significant induction of at least 2-fold changes. It is known that p38 MAPK phosphorylates DDIT3 to enhance its ability to function as a transcriptional activator (Wang and Ron, 1996; Verfaillie et al., 2010). In addition, the expression of GADD45-like proteins is known to be cytotoxic. GADD45-like proteins bind to and activate the MTK1 MAPKKK, which is upstream of both the p38 and JNK MAPKs (Takekawa and Saito, 1998). Thus, the activation of p38 MAPK by expression of the GADD45-like proteins is thought to be an indirect effect of their cytotoxicity (Takekawa and Saito, 1998).

Although PERK plays a particularly important role in mediating the activation of p38 MAPK and phosphorylation of eIF2α upon disruption of ER calcium homeostasis, it was just slightly up-regulated in this study (Liang et al., 2006; Teske et al., 2011). There was also some uncertainty on why tunicamycin did not induce the phosphorylation of PERK in the same experiment, suggesting that the effects of tunicamycin may be cell-specific. Thus, the exact role of PERK in 14-DDA induced ER-stress cannot be clearly defined at this point of time. ER stress transcription factors such as ATF4 and DDIT3 have been demonstrated to bind to the promoter of a set of autophagy genes, thereby upregulating the transcription of those genes that are involved in the formation, elongation and function of the autophagosome (B'Chir et al., 2013). The slight up-regulation of ATF4 mRNA expression as demonstrated in this study may have been enhanced by eIF2α phosphorylation.

The expression of DDIT3 is the decisive factor in determining cell's fate during ER stress and it has been identified as the key player in mediating the anti-tumor effects of ER stress-inducing agents (Oyadomari and Mori, 2004; Schonthal, 2009; Schonthal, 2013). Much emphasis has been placed on DDIT3's role as pro-apoptotic transcription factor (Oyadomari and Mori, 2004). Nonetheless, recent studies unravel another impactful role of DDIT3 as pro-autophagic transcription factor (Rouschop et al., 2010; Avivar-Valderas et al., 2011; B'Chir et al., 2013). Interestingly, the mRNA and protein expression of DDIT3 was significantly induced in 14-DDA-treated cells. Results in this study indicated that 14-DDA enhances the transcriptional activity of DDIT3 via p38 MAPK, which indicated that that DDIT3 could be an important molecule in mediating the effect of ER stress and/or autophagy in T-47D cells. This was supported with the observation that DDIT3 knockdown suppressed the formation of both ER vacuoles and autophagosomes, clearly suggests that 14-DDA-induced ER stress and autophagy is dependent on this transcription factor and that the role of DDIT3 in this situation is likely pro-autophagic.

In conclusion, 14-DDA induces ER stress-mediated autophagy in T-47D cells possibly via the GADD45A/p38 MAPK/DDIT3 pathway. However, the role of PERK, eIF2α and ATF4 remain non-conclusive. Based on these mechanistic toxicology properties, 14-DDA, as a potential ER stress inducer, may be useful as a component in the complementary medicine for use in cancer.

Conflict of interests

The authors declare no conflict of interests with respect to the research, authorship, and/or publication of this article.

Transparency document

The Transparency document associated with this article can be found, in online version.

Acknowledgements

The authors would like to acknowledge Prof. Masanori Kuroyanagi and Prof Noboru Mizushima. This fundamental work was supported in parts by the FRGS Grant (Fasa1/2013), R&D Initiatives and Sciencefund Grant (02-05-23-SF0002) awarded to TML. The authors would like to acknowledge MyBrain15 program for sponsoring THK.

Supplementary data related to this article can be found at Data in Brief (Tan et al., 2016).

References

Appenzeller-Herzog, C., Hall, M.N., 2012. Bidirectional crosstalk between endoplasmic reticulum stress and mTOR signaling. Trends Cell Biol. 22, 274–282.

Avivar-Valderas, A., Salas, E., Bobrovnikova-Marjon, E., Diehl, J.A., Nagi, C., Debnath, J., Aguirre-Ghiso, J.A., 2011. PERK integrates autophagy and oxidative stress responses to promote survival during extracellular matrix detachment. Mol. Cell. Biol. 31, 3616–3629.

Barth, S., Glick, D., Macleod, K.F., 2010. Autophagy: assays and artifacts. J. Pathol. 221, 117–124.

Bauvy, C., Meijer, A.J., Codogno, P., 2009. Assaying of autophagic protein degradation. Methods Enzymol. 452, 47–61.

B'Chir, W., Maurin, A.C., Carraro, V., Averous, J., Jousse, C., Muranishi, Y., Parry, L., Stepien, G., Fafournoux, P., Bruhat, A., 2013. The eIF2alpha/ATF4 pathway is essential for stress-induced autophagy gene expression. Nucleic Acids Res. 41, 7683–7699.

Boyd, M.R., Paull, K.D., Rubinstein, L.R., 1992. Data display and analysis strategies for the NCI disease-oriented in vitro antitumor drug screen. In: Valeriote, F.A., Corbett, T.H., Baker, L.H. (Eds.), Cytotoxic Anticancer Drugs: Models and Concepts for Drug Discovery and Development. Kluwer Academic Publishers, Massachusetts, pp. 11–34.

Decuypere, J.P., Kindt, D., Luyten, T., Welkenhuyzen, K., Missiaen, L., De Smedt, H., Bultynck, G., Parys, J.B., 2013. mTOR-controlled autophagy requires intracellular Ca (2+) signaling. PLoS One 8, e61020.

Ekalaksananan, T., Sookmai, W., Fangkham, S., Pientong, C., Aromdee, C., Seubsasana, S., Kongyingyoes, B., 2015. Activity of andrographolide and its derivatives on HPV16 pseudovirus infection and viral oncogene expression in cervical carcinoma cells. Nutr. Cancer 67, 687–696.

Fayard, E., Tintignac, L.A., Baudry, A., Hemmings, B.A., 2005. Protein kinase B/Akt at a glance. J. Cell Sci. 118, 5675–5678.

Fortier, A.-M., Asselin, E., Cadrin, M., 2011. Functional specificity of Akt isoforms in cancer progression. BioMol Concepts 2, 1–11.

Frederick, R., Mawson, C., Kendall, J.D., Chaussade, C., Rewcastle, G.W., Shepherd, P.R., Denny, W.A., 2009. Phosphoinositide-3-kinase (PI3K) inhibitors: identification of new scaffolds using virtual screening. Bioorg. Med. Chem. Lett. 19, 5842–5847.

Galluzzi, L., De Santi, M., Crinelli, R., De Marco, C., Zaffaroni, N., Duranti, A., Brandi, G., Magnani, M., 2012. Induction of endoplasmic reticulum stress response by the indole-3-carbinol cyclic tetrameric derivative CTet in human breast cancer cell lines. PLoS One 7, e43249.

Garber, K., 2009. Targeting mTOR: something old, something new. J. Natl. Cancer Inst. 101, 288–290.

Guan, S.P., Kong, L.R., Cheng, C., Lim, J.C., Wong, W.S., 2011. Protective role of 14-deoxy-11,12-didehydroandrographolide, a noncytotoxic analogue of andrographolide, in allergic airway inflammation. J. Nat. Prod. 74, 1484–1490.

Healy, S.J., Gorman, A.M., Mousavi-Shafaei, P., Gupta, S., Samali, A., 2009. Targeting the endoplasmic reticulum-stress response as an anticancer strategy. Eur. J. Pharmacol. 625, 234–246.

Hetz, C., 2012. The unfolded protein response: controlling cell fate decisions under ER stress and beyond. Nat. Rev. Mol. Cell Biol. 13, 89–102.

Hiramatsu, N., Joseph, V.T., Lin, J.H., 2011. Monitoring and manipulating mammalian unfolded protein response. Methods Enzymol. 491, 183–198.

Jarukamjorn, K., Nemoto, N., 2008. Pharmacological aspects of *Andrographis paniculata* on health and its major diterpenoid constituent andrographolide. J. Health Sci. 54, 370–381.

Jayakumar, T., Hsieh, C.-Y., Lee, J.-J., Sheu, J.-R., 2013. Experimental and clinical pharmacology of *Andrographis paniculata* and its major bioactive phytoconstituent andrographolide. Evid. Based Complement. Alternat. Med. 2013, 16.

Kabeya, Y., Mizushima, N., Ueno, T., Yamamoto, A., Kirisako, T., Noda, T., Kominami, E., Ohsumi, Y., Yoshimori, T., 2000. LC3, a mammalian homologue of yeast Apg8p, is localized in autophagosome membranes after processing. EMBO J. 19, 5720–5728.

Kondo, Y., Kanzawa, T., Sawaya, R., Kondo, S., 2005. The role of autophagy in cancer development and response to therapy. Nat. Rev. Cancer 5, 726–734.

Konishi, H., Matsuzaki, H., Tanaka, M., Ono, Y., Tokunaga, C., Kuroda, S., Kikkawa, U., 1996. Activation of RAC-protein kinase by heat shock and hyperosmolarity stress through a pathway independent of phosphatidylinositol 3-kinase. Proc. Natl. Acad. Sci. U. S. A. 93, 7639–7643.

Konishi, H., Matsuzaki, H., Tanaka, M., Takemura, Y., Kuroda, S., Ono, Y., Kikkawa, U., 1997. Activation of protein kinase B (Akt/RAC-protein kinase) by cellular stress and its association with heat shock protein Hsp27. FEBS Lett. 410, 493–498.

Kroemer, G., Galluzzi, L., Brenner, C., 2007. Mitochondrial membrane permeabilization in cell death. Physiol. Rev. 87, 99–163.

Lee, S., Morita, H., Tezuka, Y., 2015. Preferentially cytotoxic constituents of *Andrographis paniculata* and their preferential cytotoxicity against human pancreatic cancer cell lines. Nat. Prod. Commun. 10, 1153–1158.

Liang, S.H., Zhang, W., McGrath, B.C., Zhang, P., Cavener, D.R., 2006. PERK (eIF2alpha kinase) is required to activate the stress-activated MAPKs and induce the expression of immediate-early genes upon disruption of ER calcium homoeostasis. Biochem. J. 393, 201–209.

Lim, J.C., Chan, T.K., Ng, D.S., Sagineedu, S.R., Stanslas, J., Wong, W.S., 2012. Andrographolide and its analogues: versatile bioactive molecules for combating inflammation and cancer. Clin. Exp. Pharmacol. Physiol. 39, 300–310.

Liu, P., Cheng, H., Roberts, T.M., Zhao, J.J., 2009. Targeting the phosphoinositide 3-kinase pathway in cancer. Nat. Rev. Drug Discov. 8, 627–644.

Meggio, F., Donella Deana, A., Ruzzene, M., Brunati, A.M., Cesaro, L., Guerra, B., Meyer, T., Mett, H., Fabbro, D., Furet, P., et al., 1995. Different susceptibility of protein kinases to staurosporine inhibition. Kinetic studies and molecular bases for the resistance of protein kinase CK2. Eur. J. Biochem. 234, 317–322.

Mizushima, N., Yoshimori, T., Levine, B., 2010. Methods in mammalian autophagy research. Cell 140, 313–326.

Nawrocki, S.T., Carew, J.S., Dunner Jr., K., Boise, L.H., Chiao, P.J., Huang, P., Abbruzzese, J.L., McConkey, D.J., 2005. Bortezomib inhibits PKR-like endoplasmic reticulum (ER) kinase and induces apoptosis via ER stress in human pancreatic cancer cells. Cancer Res. 65, 11510–11519.

O'Reilly, K.E., Rojo, F., She, Q.B., Solit, D., Mills, G.B., Smith, D., Lane, H., Hofmann, F., Hicklin, D.J., Ludwig, D.L., Baselga, J., Rosen, N., 2006. mTOR inhibition induces upstream receptor tyrosine kinase signaling and activates Akt. Cancer Res. 66, 1500–1508.

Oslowski, C.M., Urano, F., 2011. Measuring ER stress and the unfolded protein response using mammalian tissue culture system. Methods Enzymol. 490, 71–92.

Oyadomari, S., Mori, M., 2004. Roles of CHOP/GADD153 in endoplasmic reticulum stress. Cell Death Differ. 11, 381–389.

Pal, I., Mandal, M., 2012. PI3K and Akt as molecular targets for cancer therapy: current clinical outcomes. Acta Pharmacol. Sin. 33, 1441–1458.

Park, S., Kim, D., Kaneko, S., Szewczyk, K.M., Nicosia, S.V., Yu, H., Jove, R., Cheng, J.Q., 2005. Molecular cloning and characterization of the human AKT1 promoter uncovers its up-regulation by the Src/Stat3 pathway. J. Biol. Chem. 280, 38932–38941.

Pfaffl, M.W., 2001. A new mathematical model for relative quantification in real-time RT-PCR. Nucleic Acids Res. 29, e45.

Pholphana, N., Rangkadilok, N., Thongnest, S., Ruchirawat, S., Ruchirawat, M., Satayavivad, J., 2004. Determination and variation of three active diterpenoids in *Andrographis paniculata* (Burm.f.) Nees. Phytochem. Anal. 15, 365–371.

Qin, L., Wang, Z., Tao, L., Wang, Y., 2010. ER stress negatively regulates AKT/TSC/mTOR pathway to enhance autophagy. Autophagy 6, 239–247.

Quan, Z., Gu, J., Dong, P., Lu, J., Wu, X., Wu, W., Fei, X., Li, S., Wang, Y., Wang, J., Liu, Y., 2010. Reactive oxygen species-mediated endoplasmic reticulum stress and mitochondrial dysfunction contribute to cirsimaritin-induced apoptosis in human gallbladder carcinoma GBC-SD cells. Cancer Lett. 295, 252–259.

Raghavan, R., Cheriyamundath, S., Madassery, J., 2014. 14-Deoxy-11,12-didehydroandrographolide inhibits proliferation and induces GSH-dependent cell death of human promonocytic leukemic cells. J. Nat. Med. 68, 387–394.

Rodon, J., Dienstmann, R., Serra, V., Tabernero, J., 2013. Development of PI3K inhibitors: lessons learned from early clinical trials. Nat Rev Clin Oncol 10, 143–153.

Rouschop, K.M., van den Beucken, T., Dubois, L., Niessen, H., Bussink, J., Savelkouls, K., Keulers, T., Mujcic, H., Landuyt, W., Voncken, J.W., Lambin, P., van der Kogel, A.J., Koritzinsky, M., Wouters, B.G., 2010. The unfolded protein response protects human tumor cells during hypoxia through regulation of the autophagy genes MAP1LC3B and ATG5. J. Clin. Invest. 120, 127–141.

Salazar, M., Carracedo, A., Salanueva, Í.J., Hernández-Tiedra, S., Lorente, M., Egia, A., Vázquez, P., Blázquez, C., Torres, S., García, S., Nowak, J., Fimia, G.M., Piacentini, M., Cecconi, F., Pandolfi, P.P., González-Feria, L., Iovanna, J.L., Guzmán, M., Boya, P., Velasco, G., 2009. Cannabinoid action induces autophagy-mediated cell death through stimulation of ER stress in human glioma cells. J. Clin. Invest. 119, 1359–1372.

Schleicher, S.M., Moretti, L., Varki, V., Lu, B., 2010. Progress in the unraveling of the endoplasmic reticulum stress/autophagy pathway and cancer: implications for future therapeutic approaches. Drug Resist. Updat. 13, 79–86.

Schonthal, A.H., 2009. Endoplasmic reticulum stress and autophagy as targets for cancer therapy. Cancer Lett. 275, 163–169.

Schonthal, A.H., 2013. Pharmacological targeting of endoplasmic reticulum stress signaling in cancer. Biochem. Pharmacol. 85, 653–666.

Sun, S.Y., Rosenberg, L.M., Wang, X., Zhou, Z., Yue, P., Fu, H., Khuri, F.R., 2005. Activation of Akt and eIF4E survival pathways by rapamycin-mediated mammalian target of rapamycin inhibition. Cancer Res. 65, 7052–7058.

Tabas, I., Ron, D., 2011. Integrating the mechanisms of apoptosis induced by endoplasmic reticulum stress. Nat. Cell Biol. 13, 184–190.

Takekawa, M., Saito, H., 1998. A family of stress-inducible GADD45-like proteins mediate activation of the stress-responsive MTK1/MEKK4 MAPKKK. Cell 95, 521–530.

Tan, M.L., Kuroyanagi, M., Sulaiman, S.F., Najimudin, N., Muhammad, T.S.T., 2005. Cytotoxic activities of major diterpenoid constituents of *Andrographis paniculata*. in a panel of human tumor cell lines. Pharm. Biol. 43, 501–508.

Tan, M.L., Tan, H.K., Oon, C.E., Kuroyanagi, M., Muhammad, T.S., 2012. Identification of genes involved in the regulation of 14-deoxy-11,12-didehydroandrographolide-induced toxicity in T-47D mammary cells. Food Chem. Toxicol. 50, 431–444.

Tan, H.K., Moad, A.I., Tan, M.L., 2014. The mTOR signalling pathway in cancer and the potential mTOR inhibitory activities of natural phytochemicals. Asian Pac. J. Cancer. Prev. 15, 6463–6475.

Tan, H.K., Muhammad, T.S.T., Tan, M.L., 2016. Cytotoxic parameters for 14-deoxy-11,12-didehydroandrographolide and DDIT3 silencing in T-47D breast carcinoma cells. Data in Brief (submitted).

Tasdemir, E., Galluzzi, L., Maiuri, M.C., Criollo, A., Vitale, I., Hangen, E., Modjtahedi, N., Kroemer, G., 2008. Methods for assessing autophagy and autophagic cell death. Methods Mol. Biol. 445, 29–76.

Teske, B.F., Wek, S.A., Bunpo, P., Cundiff, J.K., McClintick, J.N., Anthony, T.G., Wek, R.C., 2011. The eIF2 kinase PERK and the integrated stress response facilitate activation of ATF6 during endoplasmic reticulum stress. Mol. Biol. Cell 22, 4390–4405.

Turcotte, S., Giaccia, A.J., 2010. Targeting cancer cells through autophagy for anticancer therapy. Curr. Opin. Cell Biol. 22, 246–251.

van Gorp, A.G., Pomeranz, K.M., Birkenkamp, K.U., Hui, R.C., Lam, E.W., Coffer, P.J., 2006. Chronic protein kinase B (PKB/c-akt) activation leads to apoptosis induced by oxidative stress-mediated Foxo3a transcriptional up-regulation. Cancer Res. 66, 10760–10769.

van Schadewijk, A., van't Wout, E.F., Stolk, J., Hiemstra, P.S., 2012. A quantitative method for detection of spliced X-box binding protein-1 (XBP1) mRNA as a measure of endoplasmic reticulum (ER) stress. Cell Stress Chaperones 17, 275–279.

Verfaillie, T., Salazar, M., Velasco, G., Agostinis, P., 2010. Linking ER stress to autophagy: potential implications for cancer therapy. Int. J. Cell. Biol. 2010.

Wan, X., Harkavy, B., Shen, N., Grohar, P., Helman, L.J., 2007. Rapamycin induces feedback activation of Akt signaling through an IGF-1R-dependent mechanism. Oncogene 26, 1932–1940.

Wang, X.Z., Ron, D., 1996. Stress-induced phosphorylation and activation of the transcription factor CHOP (GADD153) by p38 MAP kinase. Science 272, 1347–1349.

Woehlbier, U., Hetz, C., 2011. Modulating stress responses by the UPRosome: a matter of life and death. Trends Biochem. Sci. 36, 329–337.

Wojcik, S., 2013. Crosstalk between autophagy and proteasome protein degradation systems: possible implications for cancer therapy. Folia Histochem. Cytobiol. 51, 249–264.

Yap, T.A., Garrett, M.D., Walton, M.I., Raynaud, F., de Bono, J.S., Workman, P., 2008. Targeting the PI3K-AKT-mTOR pathway: progress, pitfalls, and promises. Curr. Opin. Pharmacol. 8, 393–412.